
Positional Encoding Helps Recurrent Neural Networks Handle a Large Vocabulary

Takashi Morita¹

Abstract

This study discusses the effects of positional encoding on recurrent neural networks (RNNs) utilizing synthetic benchmarks. Positional encoding “time-stamps” data points in time series and complements the capabilities of Transformer neural networks, which lack an inherent mechanism for representing the data order. By contrast, RNNs can encode the temporal information of data points on their own, rendering their use of positional encoding seemingly “redundant”. Nonetheless, empirical investigations reveal the effectiveness of positional encoding even when coupled with RNNs, specifically for handling a large vocabulary that yields diverse observations. These findings pave the way for a new line of research on RNNs, concerning the combination of input-driven and autonomous time representation. Additionally, biological implications of the computational/simulation results are discussed, in the light of the affinity between the sinusoidal implementation of positional encoding and neural oscillations in biological brains.

1. Introduction

Since their invention in 2017, Transformer neural networks (Vaswani et al., 2017) have taken over as the gold standard processor/generator of time series data, from the more traditional models in the form of recurrent neural networks (RNNs; Elman, 1990). One of the most striking differences between the two models is the way they represent the temporal information of the data (i.e., the order of individual data points, or *tokens*, in the time series). On the one hand, RNNs encode temporal information by updating their internal state based on the input observations as well as the previous state. On the other hand, Transformers per se do *not* have a mechanism to represent the temporal order of data

¹Academy of Emerging Sciences, Chubu University, Kasugai, JAPAN. Correspondence to: Takashi Morita <tmorita@alum.mit.edu>.

points, so they have to rely on an external “clock” called *positional encoding*.

Positional encoding “time-stamps” input tokens through addition/concatenation of its constituent vectors to the corresponding input embeddings. In contrast to RNNs, time representation via positional encoding itself is invariant to input values (i.e., *autonomous*) until they are processed together by a network.

Although positional encoding has been considered as an *alternative* form of time representation that replaces RNNs (in combination with Transformers), positional encoding and RNNs are *not* fundamentally incompatible; that is, inputs to RNNs can be “redundantly” augmented by position-encoding vectors. Indeed, autonomous activities of biological neurons and other organs are thought to play an important role in time perception (Matell & Meck, 2004; Buhusi & Meck, 2005), as well as other perceptual processes (including vision; Milner, 1974; Eckhorn et al., 1988; Gray et al., 1989; and odors; Milner, 1974; Eckhorn et al., 1988; Gray et al., 1989; Wehr & Laurent, 1996; Perez-Orive et al., 2002) and motor control (Marder & Bucher, 2001; Gross et al., 2002; Proctor et al., 2010).

Accordingly, the present study explores “redundant” positional encoding on inputs to RNNs through synthetic benchmarks. The experiments will unveil that positional encoding aids RNNs in handling a wider variety of discrete inputs (i.e., a larger vocabulary) than those without positional encoding.

The contributions of this study are summarized as follows:

- Empirical benefits of positional encoding coupled with RNNs are demonstrated. These findings pave the way for a new line of research on RNNs, regarding the combination of input-driven and autonomous time representation.
- The specific implementation of positional encoding in this study takes the form of sinusoidal waves (Vaswani et al., 2017), which have an affinity to neural oscillations in biological brains. Accordingly, the present study will also lead to a deeper understanding

of the functionalities of biological rhythms.

2. Related Works

2.1. Theoretical and Empirical Computational Power of RNNs

Mathematically, RNNs are known to be Turing-complete; they can simulate Turing machines if their weights have infinite precision and are ideally tuned¹ (Siegelmann & Sontag, 1992; 1994; 1995; Siegelmann, 1996; 1999; Chen et al., 2018). Indeed, even RNNs with random recurrent and input-to-hidden weights (called *reservoir computers*; Maass et al., 2002; Jaeger & Haas, 2004) can achieve the universal approximation property when their hidden-to-output weights are idealized (Grigoryeva & Ortega, 2018; Gonon & Ortega, 2020). These theoretical results motivate the use of RNNs for processing complex time series such as human languages (Sundermeyer et al., 2012; Graves, 2013) and weather (Shi et al., 2015).

In practice, however, RNN weights are bounded by finite precision and must be optimized based on finite observations of data. These settings impose limitations on the empirical capabilities of RNNs (Chen et al., 2018; Weiss et al., 2018). For example, empirical RNNs cannot store infinitely many observations in their memory, or state vector(s), and the memorized information decays over time. This latter problem with the memory duration has attracted the interest of researchers, leading to extensive exploration of RNN architectures for a longer-lasting memory (Hochreiter & Schmidhuber, 1997; Arjovsky et al., 2016; Neil et al., 2016; Chang et al., 2017; Jing et al., 2017; 2019; Voelker et al., 2019; Gu et al., 2020).

More specifically, the previous studies evaluated the memory capacity of RNNs using a three-phase task (called the *copying memory task*; Arjovsky et al., 2016; a schematic illustration of the task is provided in Fig. 10 in Appendix C.1):

1. **Copy:** A sequence of random integers $x_1, \dots, x_L \in \{1, \dots, K\}$ is fed to the model under evaluation (where L and K denote the input length and vocabulary size respectively).
2. **Hold:** The model does nothing but hold the input information against its memory decay for some time steps T .

¹In order to be Turing-complete, RNNs must also be allowed to read an entire input prior to their output emission; they are at most context-sensitive if they have to return an output at each time step upon the receipt of an input token (Chen et al., 2018; Weiss et al., 2018).

3. **Paste:** The model reconstructs the input sequence as precisely as possible. The model is evaluated by the quality of this reconstruction (quantified by the accuracy or cross-entropy loss).

The major interest has been put in the length T of the “hold” phase—evaluating the memory *duration* of RNNs—while the input length L and the vocabulary size K were typically set small ($L = 10, K = 8$; Arjovsky et al., 2016; Neil et al., 2016; Chang et al., 2017; Jing et al., 2017; 2019; Voelker et al., 2019; Gu et al., 2020). By contrast, the present study explores a larger vocabulary size up to $K = 16,384$ (as well as longer input sequences, with $L = 64$ by default, while setting $T = 0$ for simplicity), thereby measuring the ability of RNNs to handle a wider variety of input patterns (with vs. without the aid of positional encoding).²

In terms of practical applications, RNNs have recently been replaced by Transformer networks in various domains (Vaswani et al., 2017). One of the major advantages of Transformers over RNNs is in their ability to handle longer dependencies among input tokens, due to their memory-free architecture for information retrieval; instead of storing past information by updating a fixed-sized vector, Transformers re-observe all the past tokens (up to an empirical bound) and compute their contribution for each time step. For example, in the language modeling task (i.e., autoregressive prediction of individual tokens in sentences), a Transformer can exploit information from the past 900 tokens, whereas a long short-term memory (LSTM; Hochreiter & Schmidhuber, 1997) can only rely on 200–400 tokens (Khandelwal et al., 2018; Dai et al., 2019).

2.2. Positional Encoding

Positional encoding is a high-dimensional representation of temporal structures in input data (Gehring et al., 2017). The primary demand for this representation scheme comes from Transformers. Unlike RNNs, Transformers lack an inherent mechanism for representing input arrangements. Accordingly, input tokens to a Transformer are “time-stamped” via addition/concatenation of a position-encoding vector.

In the original implementation of Transformer, token positions were encoded by sinusoidal waves of various predefined frequencies (Vaswani et al., 2017). While this original encoding scheme is powerful enough for a wide range of tasks, researchers have explored for other possibilities as well. For example, the well-known BERT pretraining for natural language processing employed learnable em-

²The standard copying memory task is also tested in Appendix C.1.

beddings to encode token positions (Devlin et al., 2019). Some studies also suggested that the combination of the sinusoidal and learnable encoding improves model performance (Dai et al., 2019). There is also an option to encode the *distance* between tokens rather than the elapsed time from the sequence onset (Shaw et al., 2018; Dai et al., 2019).

Besides Transformers, positional encoding is also used to represent the elapsed time in diffusion processes (Ho et al., 2020; Song et al., 2021). Moreover, the effectiveness of positional encoding is not limited to *temporal* information; previous studies in three-dimensional mesh/point-cloud modeling report that sinusoidal transformation of *spatial* data improves model performance compared to the raw coordinate representation (Mildenhall et al., 2020; Jun & Nichol, 2023).

Despite the widespread use of positional encoding in various areas of machine learning today, its applications to pure RNNs remain largely unexplored. To the best of the author’s knowledge, there are only two previous studies that benchmarked position-encoded RNNs. On the one hand, Karanikolos & Refanidis (2019) reported that a position-encoded LSTM outperformed a vanilla LSTM and a small Transformer (with four layers) in text summarization. On the other hand, Vincent-Lamarre et al. (2016)—prior to the proposal of sinusoidal positional encoding in the deep learning community—discovered that oscillatory signals at random frequencies enhance the performance of a random RNN (i.e., reservoir computer) in the timing task; this task benchmarks the memory duration of a model by first feeding it with an input pulse and then having it draw a sharp Gaussian (smoothed output pulse) after a specific interval of time. In other studies, positional encoding and RNNs served as submodules within a more complex model, typically in conjunction with an attention mechanism (Kim et al., 2018; Song et al., 2020).

Similarly, the time index in time series data has rarely been coupled with RNNs, presumably because of its “redundancy” along the functionality of RNNs. As an exception, Neil et al. (2016) proposed a periodic gating mechanism for updating the state and memory cell of LSTM. This periodic gating was scheduled according to a triangular wave interspersed with a plateau at the floor value ($= 0.0$; the frequency, phase, and the duration of the wave phase were learnable parameters).

2.3. Computational Neuroscience

As noted in the previous section, sinusoidal waves are the gold standard implementation of positional encoding. Remarkably, time representation in biological brains has also been modeled by the cyclic activities of neurons. Miall (1989) first demonstrated that a bundle of oscillators with

varying frequencies can encode arbitrary time intervals when they are read out by a single output neuron trained by the Hebbian rule. Matell & Meck (2004) subsequently furnished a biological interpretation of this model (with further refinements). Specifically, the model can be seen as the cortico-striatal network, in which oscillatory signals from the cortical neurons with frequency variations are filtered/selected by the striatal neurons that are reinforced to fire at specific timings.

More recently, Kawai et al. (2023) proposed a backpropagation-free RNN (a variant of reservoir computers; Maass et al., 2002; Jaeger & Haas, 2004) that generates a bundle of limit cycles with diverse frequencies and phases (as well as waveforms). These limit cycles serve as rich input signals for a linear readout layer, and the model achieved twenty times longer memory duration (assessed via the timing task) than the previous gold standard model (Laje & Buonomano, 2013).

3. Methods

3.1. Task

This study inquired into the effect of positional encoding on RNNs through the reverse-ordering task (Fig. 1). Given a sequence of random integers, the network was trained to reconstruct them in reverse order (e.g. $8, 29, 2, 11 \mapsto 11, 2, 29, 8$). Unlike the copying memory task (see Appendix C.1 for the results of this task; Arjovsky et al., 2016), the input and output phases were *not* interrupted by a “hold” phase wherein the model simply retains the information without receiving additional information or returning outputs.

The use of the reverse-ordered target sequences was intended to mitigate the inherent suitability of the sinusoidal positional encoding (see §3.2) for the simple reconstruction in the original input order. Without changing the order of the target sequences, position-encoded RNNs might simply learn to shift the phase of the sinusoidal timestamp on each input token and align it with the timestamp on the corresponding output query. By contrast, more complex processing of the positional encoding is required for RNNs to solve the reverse-ordering, since the distance between the inputs and outputs in correspondence is not constant.

Besides the reverse-ordering task, two additional benchmarks are discussed in Appendix C to further investigate the effect of positional encoding on RNNs.

3.2. Model Architecture

The task presented in the previous section was processed by single-layer RNNs. Three major variants of RNNs were investigated here: (i) the naive RNN orig-

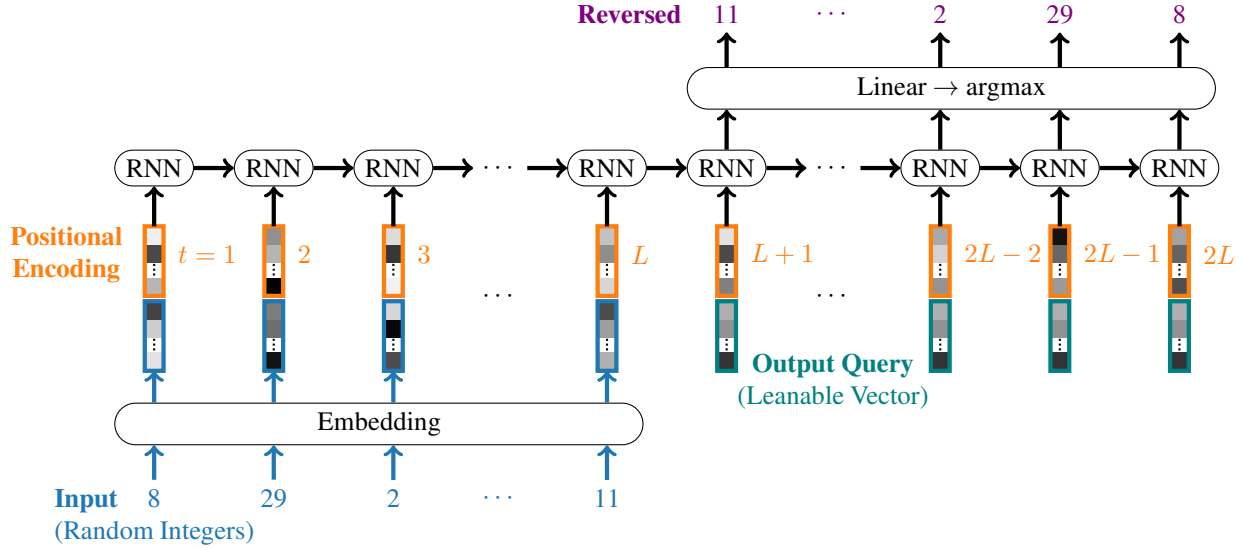


Figure 1. Model structure and task illustration.

inally proposed by Elman (1990), (ii) the gated recurrent unit (GRU; Cho et al., 2014), and (iii) the LSTM (Hochreiter & Schmidhuber, 1997).

Each of the integers in the input sequences was first embedded and concatenated with the positional encoding, and then fed to the RNN. This study adopted the canonical sinusoidal positional encoding designed for Transformers (Vaswani et al., 2017); specifically, each time step t was encoded by the D_{pos} -dimensional vector, $(PE_{t,1}, \dots, PE_{t,D_{pos}})^T$, defined as follows:³

$$PE_{t,2i} := \sin\left(\frac{t-1}{10000^{\frac{2(i-1)}{D_{pos}}}}\right) / \sqrt{\frac{D_{pos}}{2}} \quad (1)$$

$$PE_{t,2i+1} := \cos\left(\frac{t-1}{10000^{\frac{2(i-1)}{D_{pos}}}}\right) / \sqrt{\frac{D_{pos}}{2}} \quad (2)$$

For the sake of learning stability, the positional encoding was divided by $\sqrt{D_{pos}/2}$ so that the encoding vectors had the unit L2-norm. Note that the time step t increased throughout both the input and output phases (i.e., $t = 1, \dots, L, L+1, \dots, 2L$ where L represents the input length), without any hard-coded association between the input and output positions.

After reading the entire input sequence, the network received a command to return the output. This command was represented in the form of a time-invariant learnable vector,

³The adjustment of the time and frequency indices (“ $t-1$ ” and “ $i-1$ ”) in Eqs. 1 and 2 aligns the 1-based indexing in this paper (adopted for better readability) with the 0-based indexing in Python.

and fed to the RNN in place of the input embedding (cf. Arjovsky et al., 2016). The outputs from the RNN module were linearly projected into the classification logits, whose cross-entropy loss against the target sequence was used to optimize the entire network. Model predictions in the testing phase were defined by the argmax of these logits for each time step.

Information on the hyperparameters can be found in Appendix A. The code used in this study is also available online.⁴

4. Results

4.1. Effects on Vocabulary Size vs. Input Length

Positional encoding improved the ability of RNNs to handle a larger vocabulary in the reverse-ordering task (Fig. 2). For instance, the position-encoded LSTM successfully reversed the input sequences of 64 integers (see Appendix B.1 for a discussion of robustness to variable input length) randomly drawn from the vocabulary of size 2–16,384, achieving the token-wise accuracy above 95%; the performance of the vanilla LSTM without positional encoding, by contrast, degraded as the vocabulary size increased. Similarly, the position-encoded Elman RNN and GRU outperformed those without positional encoding (except when the Elman RNN processed the vocabulary of size 8,192), albeit reaching their capacity limit at the vocabulary sizes of 128 (Elman RNN) and 512 (GRU).

In contrast to the enhancement in the manageable vocabu-

⁴The link to the online repository will be added here upon the acceptance of this paper.

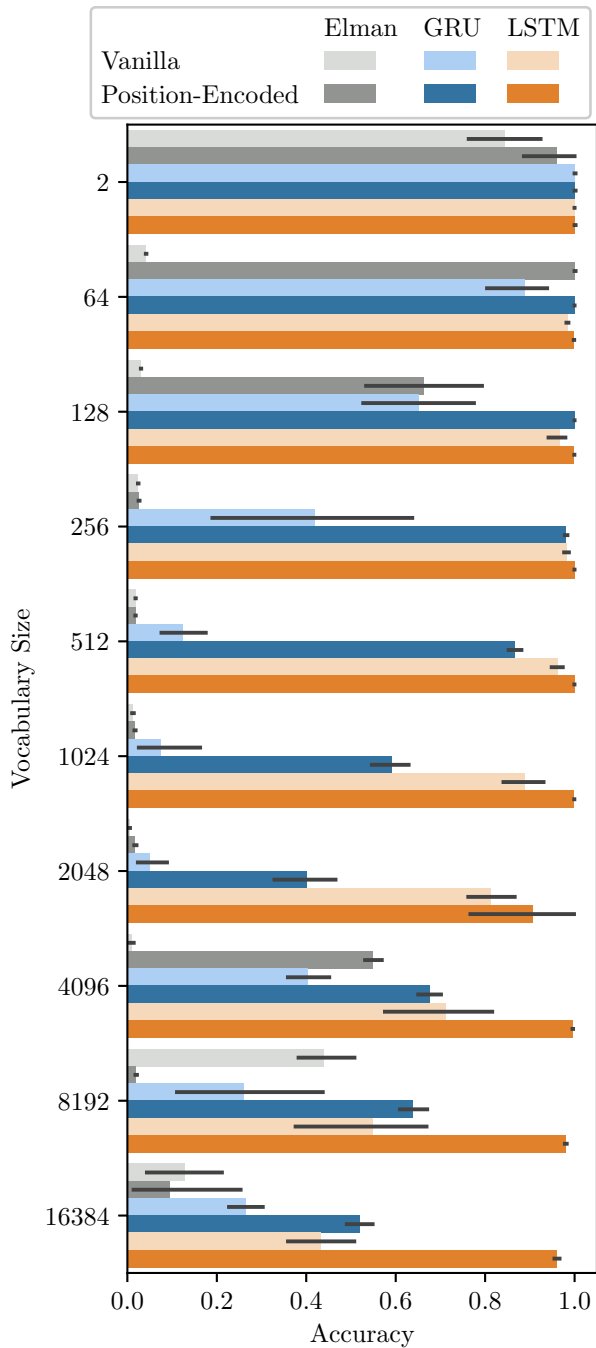


Figure 2. Token-wise accuracy of the reverse-ordering task performed by RNNs with and without positional encoding (labeled as “Position-Encoded” and “Vanilla” respectively). The input length was fixed at 64. The error bars represent the 95% confidence interval estimated from 10,000 bootstrapped samples of five training-test trials with different random seeds. Each of the five trials held out 1024 random sequences (= 65,536 tokens) for computing the test accuracy.

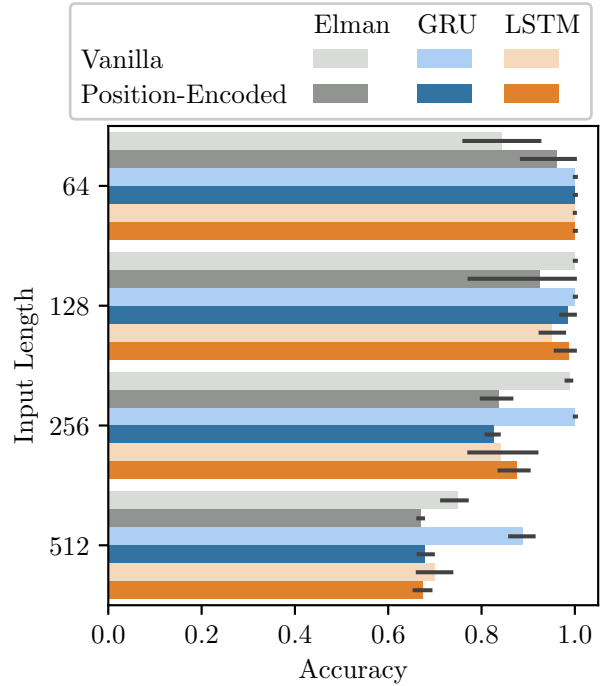


Figure 3. Token-wise accuracy of the reverse-ordering task performed by RNNs with and without positional encoding (labeled as “Position-Encoded” and “Vanilla” respectively). The vocabulary size was fixed at 2. The error bars represent the 95% confidence interval estimated from 10,000 bootstrapped samples of five training-test trials with different random seeds. Each of the five trials held out 1024 random sequences for computing the test accuracy.

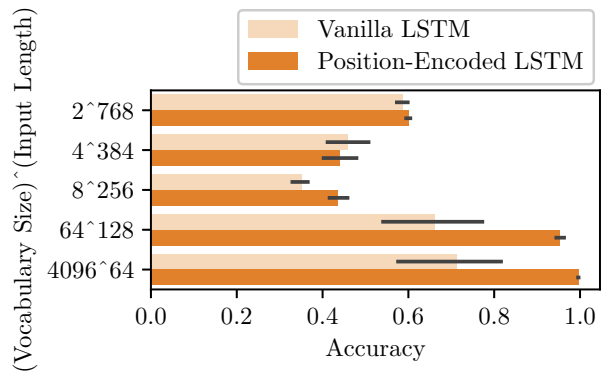


Figure 4. Token-wise accuracy of the reverse-ordering task performed by the LSTM with and without positional encoding (labeled as “Position-Encoded” and “Vanilla” respectively). The number of possible input patterns were kept constant as $K^L := 2^{796} = 4^{384} = 8^{256} = 64^{128} = 4096^{64}$, where K and L denote the vocabulary size and the input length respectively. The error bars represent the 95% confidence interval estimated from 10,000 bootstrapped samples of five training-test trials with different random seeds. Each of the five trials held out 1024 random sequences for computing the test accuracy.

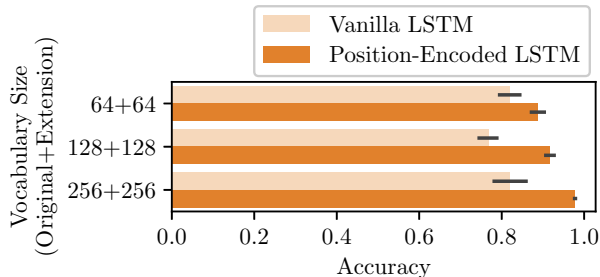


Figure 5. Token-wise accuracy of the reverse-ordering task performed by the vocabulary-extended LSTM with and without positional encoding (labeled as “Position-Encoded” and “Vanilla” respectively). The vocabulary size was doubled by extending the input-embedding and output-projection layers of pretrained networks. Only the extended weights were retrained while all the pretrained weights were frozen intact. The input length was fixed at 64. The error bars represent the 95% confidence interval estimated from 10,000 bootstrapped samples of five training-test trials with different random seeds. Each of the five trials held out 1024 random sequences per length for computing the test accuracy.

lary size, positional encoding did *not* aid RNNs in handling longer input sequences; when the vocabulary size was kept minimal ($= 2$) and the input length was increased from 64 to 512, the accuracy of the LSTM degraded regardless of the use/non-use of positional encoding (Fig. 3). Moreover, position-encoded Elman RNN and GRU scored lower accuracy than the vanilla baselines.

To further clarify the effect of positional encoding on a large vocabulary vs. long inputs, an additional experiment was performed on the LSTM where the number of possible input patterns was kept constant at $K^L := 2^{796} = 4^{384} = 8^{256} = 64^{128} = 4096^{64}$, trading off the vocabulary size K vs. the input length L . This experiment confirmed that the contribution of positional encoding was greater for a larger vocabulary size K than for a greater input length L (Fig. 4).

4.2. Vocabulary Extension

An intuitive hypothesis on the improvement in the manageability of large vocabularies is that the position-encoded RNN learned the general rule governing the reverse-ordering task, abstracted away from the individual tokens. The sequence-to-sequence mapping can be schematized as $x_1, \dots, x_L \mapsto x_L, \dots, x_1$, and “intelligent” agents aware/informed of this rule—like humans—would be able to generalize it to new vocabulary items.

In order to investigate this hypothesis, *vocabulary extension* was attempted on the LSTM. Specifically, additional weights were appended to the input-embedding and output-projection layers of the pretrained network in order to ac-

commodate extra vocabulary items. Note that the pretrained weights (i.e., the recurrent/gating weights of the RNN as well as the input-embedding and output-projection weights for the original vocabulary items) were frozen intact, and only the additional weights were optimized for the new observations including both the original and extra vocabulary items.

As a result, the vocabulary extension was more successful with than without positional encoding (Fig. 5). While the difference between the two networks was marginal when they learned the vocabulary of size 128–512 from scratch (Fig. 2), the advantage of the positional encoding became evident when they learned the vocabulary of the same size through extension.

5. Discussions

5.1. Summary of Findings and Technical Discussions

The experiment in this study demonstrated that positional encoding enhances the ability of RNNs to handle a large vocabulary (see also Appendix C.2 for similar results based on a different benchmark, and Appendix B.3 for the *inapplicability* of the enhancement to an “infinite” vocabulary). This finding is enlightening as RNNs were designed for processing time series data on their own and, thus, presumed to function without recourse to an “external clock”—at least in principle—unlike Transformers (Siegelmann & Sontag, 1992; 1994; 1995; Siegelmann, 1996; 1999). The results of the present study suggest that positional encoding does *not* conflict with the input-driven temporal representation of RNNs, but rather enhances/complements their capabilities.

Unlike the input-driven representation of temporal information in RNNs, positional encoding is *autonomous* and invariant to input values. Consequently, positional encoding would be useful for discovering general patterns (e.g., reverse ordering) behind individually diverse observations (e.g., random samples from a large vocabulary). This view of positional encoding is also supported by the experiment on the vocabulary extension (§4.2), where the position-encoded LSTM achieved higher accuracies than the vanilla baseline, even though they almost tied in their learning of the equally large vocabularies from scratch. Once RNNs capture the general rule governing the task with the assistance of positional encoding, the only subsequent work is to update their “dictionary” to accommodate new vocabulary items.

The improvement provided by the positional encoding, however, was confined to the manageable vocabulary size. Specifically, the positional encoding did not help RNNs handle longer inputs (nor extend their memory duration, as shown in Appendix C.1). While alternative forms of po-

sitional encoding may eventually prove to enhance these capacities, the refinement of network architectures—as explored in the previous studies (Hochreiter & Schmidhuber, 1997; Arjovsky et al., 2016; Neil et al., 2016; Chang et al., 2017; Jing et al., 2017; 2019; Voelker et al., 2019; Gu et al., 2020)—would remain a more promising avenue for achieving longer-lasting memory.

5.2. Biological Implications

The present study adopted the gold-standard implementation of positional encoding designed for Transformers, which encoded token positions with sinusoidal waves whose frequencies ranged in a geometric progression (Eqs. 1, 2; Vaswani et al., 2017). The idea of representing time with cyclic signals has an affinity with computational modeling of biological brains. Specifically, Miall (1989) highlighted that a combination of non-harmonic waves can encode longer temporal information beyond the cycles of the individual waves; the cycle of the entire wave bundle is defined by the least common multiple of the individuals, and becomes longer as more waves are included in the bundle. Thus, biological neurons or their ensembles—each having only a short oscillatory cycle—can collectively function as a powerful clock (Matell & Meck, 2004; Buhusi & Meck, 2005). Moreover, a combination of high-frequency waves can encode temporal information at a higher resolution than a single slow oscillation, whose change is indiscernible in a short time frame (Mildenhall et al., 2020; see also Rahaman et al., 2019).

Neural oscillations are also considered to underlie various cognitive/behavioral activities beyond their clock-like function. Milner (1974), Grossberg (1976), and von der Malsburg (1981/1994) proposed that coherent visual perception of an object is made possible by correlations among neural oscillations in spatially segregated brain regions that are responsible for different “features” of the object (including colors, shapes, and movements). This hypothesis—called *binding-by-synchrony*—was later supported by experimental and simulational studies (Eckhorn et al., 1988; Gray et al., 1989; Seth et al., 2004; see also Wehr & Laurent, 1996; Perez-Orive et al., 2002, for related studies on olfactory perception; and Shadlen & Movshon, 1999; Dong et al., 2008; Merker, 2013, for counterarguments to the hypothesis). Similarly, oscillatory neurons are thought to help coordinate movements of distinct body parts (Gross et al., 2002; Proctor et al., 2010), and also to serve as *central pattern generators* that drive rhythmic activities such as walking and breathing (Marder & Bucher, 2001). Regarding their association with memory, gamma and theta oscillations (25–100 Hz and 4–8 Hz respectively) are considered to establish communication between the hippocampus

and the cortex for encoding/decoding episodic memories (Teyler & DiScenna, 1986; Klimesch, 1996; Başar et al., 1999; Kahana, 2006; Nyhus & Curran, 2010).

Supplementing those wide-ranging (potential) functionalities proposed in the previous studies, the computational/simulational results of the present study raise a novel hypothesis concerning the role of neural oscillations and/or other biological rhythms; input-invariant, autonomous signals may guide learners to discover general rules/patterns behind individually diverse observations. For instance, human languages follow syntactic rules that describe common patterns across individual words, and biological oscillations may anchor sentences composed of different words to such abstract patterns. Moreover, the improvement in the vocabulary extension (§4.2) suggests that learners can update their knowledge more easily through oscillation-based learning than through mere input-driven information processing.

It is pertinent to note, however, that the findings in this study hinge upon the utilization of backpropagation through time, a learning method often critiqued for its biological implausibility (Lillicrap et al., 2016; Lillicrap & Santoro, 2019). Investigation of alternative learning strategies—such as reservoir computing (Maass et al., 2002; Jaeger & Haas, 2004)—is therefore crucial in future studies to assess the biological relevance of positional encoding.

Besides the issue of the backpropagation-based learning, the primary open question left by the present study is the effectiveness of other waveforms, frequencies, and phases as implementations of positional encoding. As noted in §2.2, the exploration for superior positional encoding (with respect to Transformers) is an active field of machine learning, and future studies on position-encoded RNNs should also consider their biological plausibility. Specifically, the standard sinusoidal positional encoding (Eqs. 1, 2) appears to be over-idealized for biological modeling; for example, the concatenation of sine and cosine waves keeps the L2-norm of the encoding vectors constant over time, which is *not* guaranteed for neural oscillations. For instance, the alpha waves (8–12 Hz) are known to exhibit higher positive amplitudes (crest) than negative amplitudes (trough), and are thus non-sinusoidal (Stam et al., 1999; Nikulin et al., 2007; 2010; Mazaheri & Jensen, 2008). Some (or many) of the sinusoidal waves in the positional encoding were also notably long—spanning up to $20,000\pi$ time steps—as they were tailored to capture long-distance dependencies in human languages. And the specific choice of geometrically progressive wave frequencies lacks biological justification, necessitating further exploration of alternative frequency combinations for future studies.

Moreover, the source of the oscillatory signals should not

be left as an assumption, but rather should be modeled by a neural network (and/or by a simulation of other organs). Recently, Kawai et al. (2023) proposed a variant of RNNs that generates a bundle of limit cycles with distinct waveforms, frequencies, and/or phases. Their network autonomously produces cyclic signals after receiving an initial impulsive input, without additional driving force from subsequent inputs. In their study, the generated signals were processed by a single linear layer (i.e., in the paradigm of reservoir computing; Maass et al., 2002; Jaeger & Haas, 2004). However, in principle, the model can be connected to another RNN, serving as positional encoding.

Finally, it is noteworthy that (absolute) positional encoding is typically aligned with the onset of a given task, with the initial tokens of different sequences all indexed as $t = 1$ (or 0). Biologically, this setup implies that the phase of neural oscillations is reset at the beginning of a specific task. Although such phase initialization has indeed been attested in experimental studies (Zugaro et al., 2005), biological agents are constantly exposed to diverse stimuli and tasks in the real world, making it impractical to reset the oscillations for each one. Interestingly, however, previous studies on Transformers have shown that random phase shifts in the sinusoidal positional encoding do not impair, but rather enhance the adaptability of the networks to long data beyond their experience during training (Kiyono et al., 2021; Ruoss et al., 2023). Appendix B.1 of this study also reports that the position-encoded LSTM is robust to input-length perturbations (i.e., uncertain onset time of the output phase) in the reverse-ordering task. Hence, strict alignment may not be a prerequisite for the effective utilization of positional encoding or neural oscillations if their processor is powerful enough.

6. Conclusion

This study explored a seemingly “redundant” combination of RNNs and positional encoding, and discovered its superiority over vanilla RNNs in handling a larger vocabulary. Although RNNs have been replaced by Transformers in a variety of practical applications, their study retains significance from biological standpoints. Moreover, the sinusoidal positional encoding has a noticeable affinity to theories of time representation in biological neural networks. Hence, the findings here open a new venue for the study of RNNs.

Acknowledgements

This study was supported by JST ACT-X (JPMJAX21AN) and Core Research for Evolutional Science and Technology (JPMJCR17A4), JSPS Grant-in-Aid for Early-Career Scientists (JP21K17805) and for Scientific Re-

search (JP22H03914), and Kayamori Foundation of Informational Science Advancement (K35XXVIII620). The author also gratefully acknowledges the support of the Academic Center for Computing and Media Studies (ACCMS), Kyoto University, regarding the use of their supercomputer system.

Impact Statements

This paper presents work whose goal is to advance the field of machine learning and computational neuroscience. Although there are many potential societal consequences of our work, none of them is considered to deserve special highlights beyond other standard studies in the fields.

References

- Arjovsky, M., Shah, A., and Bengio, Y. Unitary evolution recurrent neural networks. In Balcan, M. F. and Weinberger, K. Q. (eds.), *Proceedings of The 33rd International Conference on Machine Learning*, volume 48 of *Proceedings of Machine Learning Research*, pp. 1120–1128, New York, New York, USA, 20–22 Jun 2016. PMLR.
- Başar, E., Basar-Eroglu, C., Karakas, S., and Schürmann, M. Oscillatory brain theory: a new trend in neuroscience. *IEEE Engineering in Medicine and Biology Magazine*, 18(3):56–66, 1999. doi: 10.1109/51.765190.
- Buhusi, C. V. and Meck, W. H. What makes us tick? functional and neural mechanisms of interval timing. *Nature Reviews Neuroscience*, 6(10):755–765, 2005. doi: 10.1038/nrn1764.
- Chang, S., Zhang, Y., Han, W., Yu, M., Guo, X., Tan, W., Cui, X., Witbrock, M., Hasegawa-Johnson, M. A., and Huang, T. S. Dilated recurrent neural networks. In Guyon, I., Luxburg, U. V., Bengio, S., Wallach, H., Fergus, R., Vishwanathan, S., and Garnett, R. (eds.), *Advances in Neural Information Processing Systems*, volume 30. Curran Associates, Inc., 2017.
- Chen, Y., Gilroy, S., Maletti, A., May, J., and Knight, K. Recurrent neural networks as weighted language recognizers. In Walker, M., Ji, H., and Stent, A. (eds.), *Proceedings of the 2018 Conference of the North American Chapter of the Association for Computational Linguistics: Human Language Technologies, Volume 1 (Long Papers)*, pp. 2261–2271, New Orleans, Louisiana, June 2018. Association for Computational Linguistics. doi: 10.18653/v1/N18-1205.
- Cho, K., van Merriënboer, B., Gulcehre, C., Bahdanau, D., Bougares, F., Schwenk, H., and Bengio, Y. Learning phrase representations using RNN encoder–decoder

- for statistical machine translation. In *Proceedings of the 2014 Conference on Empirical Methods in Natural Language Processing (EMNLP)*, pp. 1724–1734, Doha, Qatar, October 2014. Association for Computational Linguistics. doi: 10.3115/v1/D14-1179.
- Dai, Z., Yang, Z., Yang, Y., Carbonell, J., Le, Q., and Salakhutdinov, R. Transformer-XL: Attentive language models beyond a fixed-length context. In *Proceedings of the 57th Annual Meeting of the Association for Computational Linguistics*, pp. 2978–2988, Florence, Italy, July 2019. Association for Computational Linguistics. doi: 10.18653/v1/P19-1285.
- Devlin, J., Chang, M.-W., Lee, K., and Toutanova, K. BERT: Pre-training of deep bidirectional transformers for language understanding. In *Proceedings of the 2019 Conference of the North American Chapter of the Association for Computational Linguistics: Human Language Technologies, Volume 1 (Long and Short Papers)*, pp. 4171–4186, Minneapolis, Minnesota, June 2019. Association for Computational Linguistics. doi: 10.18653/v1/N19-1423.
- Dong, Y., Mihalas, S., Qiu, F., von der Heydt, R., and Niebur, E. Synchrony and the binding problem in macaque visual cortex. *Journal of Vision*, 8(7):30, 11 2008. ISSN 1534-7362. doi: 10.1167/8.7.30.
- Eckhorn, R., Bauer, R., Jordan, W., Brosch, M., Kruse, W., Munk, M., and Reitboeck, H. J. Coherent oscillations: A mechanism of feature linking in the visual cortex? *Biological Cybernetics*, 60(2):121–130, 1988. doi: 10.1007/BF00202899.
- Elman, J. L. Finding structure in time. *Cognitive Science*, 14(2):179–211, 1990. doi: 10.1207/s15516709cog1402-1.
- Gehring, J., Auli, M., Grangier, D., Yarats, D., and Dauphin, Y. N. Convolutional sequence to sequence learning. In Precup, D. and Teh, Y. W. (eds.), *Proceedings of the 34th International Conference on Machine Learning*, volume 70 of *Proceedings of Machine Learning Research*, pp. 1243–1252. PMLR, 06–11 Aug 2017.
- Gonon, L. and Ortega, J.-P. Reservoir computing universality with stochastic inputs. *IEEE Transactions on Neural Networks and Learning Systems*, 31(1):100–112, 2020. doi: 10.1109/TNNLS.2019.2899649.
- Graves, A. Generating sequences with recurrent neural networks. arXiv:1308.0850, 2013.
- Gray, C. M., König, P., Engel, A. K., and Singer, W. Oscillatory responses in cat visual cortex exhibit inter-columnar synchronization which reflects global stimulus properties. *Nature*, 338(6213):334–337, 1989. doi: 10.1038/338334a0.
- Grigoryeva, L. and Ortega, J.-P. Echo state networks are universal. *Neural Networks*, 108:495–508, 2018. ISSN 0893-6080. doi: 10.1016/j.neunet.2018.08.025.
- Gross, J., Timmermann, L., Kujala, J., Dirks, M., Schmitz, F., Salmelin, R., and Schnitzler, A. The neural basis of intermittent motor control in humans. *Proceedings of the National Academy of Sciences*, 99(4):2299–2302, 2002. doi: 10.1073/pnas.032682099.
- Grossberg, S. Adaptive pattern classification and universal recoding: II. feedback, expectation, olfaction, illusions. *Biological Cybernetics*, 23(4):187–202, 1976. doi: 10.1007/BF00340335.
- Gu, A., Dao, T., Ermon, S., Rudra, A., and Ré, C. HiPPO: Recurrent memory with optimal polynomial projections. In Larochelle, H., Ranzato, M., Hadsell, R., Balcan, M., and Lin, H. (eds.), *Advances in Neural Information Processing Systems*, volume 33, pp. 1474–1487. Curran Associates, Inc., 2020.
- Ho, J., Jain, A., and Abbeel, P. Denoising diffusion probabilistic models. In Larochelle, H., Ranzato, M., Hadsell, R., Balcan, M., and Lin, H. (eds.), *Advances in Neural Information Processing Systems*, volume 33, pp. 6840–6851. Curran Associates, Inc., 2020.
- Hochreiter, S. and Schmidhuber, J. Long short-term memory. *Neural Computation*, 9(8):1735–1780, 1997. ISSN 0899-7667. doi: 10.1162/neco.1997.9.8.1735.
- Jaeger, H. and Haas, H. Harnessing nonlinearity: Predicting chaotic systems and saving energy in wireless communication. *Science*, 304(5667):78–80, 2004. ISSN 0036-8075. doi: 10.1126/science.1091277.
- Jing, L., Shen, Y., Dubcek, T., Peurifoy, J., Skirlo, S., LeCun, Y., Tegmark, M., and Soljačić, M. Tunable efficient unitary neural networks (EUNN) and their application to RNNs. In Precup, D. and Teh, Y. W. (eds.), *Proceedings of the 34th International Conference on Machine Learning*, volume 70 of *Proceedings of Machine Learning Research*, pp. 1733–1741. PMLR, 06–11 Aug 2017.
- Jing, L., Gulcehre, C., Peurifoy, J., Shen, Y., Tegmark, M., Soljagic, M., and Bengio, Y. Gated orthogonal recurrent units: On learning to forget. *Neural Computation*, 31(4): 765–783, 2019. doi: 10.1162/neco_a-01174.
- Jun, H. and Nichol, A. Shap-E: Generating conditional 3D implicit functions, 2023.
- Kahana, M. J. The cognitive correlates of human brain oscillations. *Journal of Neuroscience*, 26(6):1669–1672,

2006. ISSN 0270-6474. doi: 10.1523/JNEUROSCI.3737-05c.2006.
- Karanikolos, A. and Refanidis, I. Encoding position improves recurrent neural text summarizers. In Abbas, M. and Freihat, A. A. (eds.), *Proceedings of the 3rd International Conference on Natural Language and Speech Processing*, pp. 142–150, Trento, Italy, September 2019. Association for Computational Linguistics.
- Kawai, Y., Park, J., Tsuda, I., and Asada, M. Learning long-term motor timing/patterns on an orthogonal basis in random neural networks. *Neural Networks*, 163:298–311, 2023. ISSN 0893-6080. doi: 10.1016/j.neunet.2023.04.006.
- Khandelwal, U., He, H., Qi, P., and Jurafsky, D. Sharp nearby, fuzzy far away: How neural language models use context. In *Proceedings of the 56th Annual Meeting of the Association for Computational Linguistics (Volume 1: Long Papers)*, pp. 284–294, Melbourne, Australia, July 2018. Association for Computational Linguistics. doi: 10.18653/v1/P18-1027.
- Kim, J.-S., Kim, J., Park, S., Lee, K., and Lee, Y. Modeling with recurrent neural networks for open vocabulary slots. In Bender, E. M., Derczynski, L., and Isabelle, P. (eds.), *Proceedings of the 27th International Conference on Computational Linguistics*, pp. 2778–2790, Santa Fe, New Mexico, USA, August 2018. Association for Computational Linguistics.
- Kingma, D. P. and Ba, J. Adam: A method for stochastic optimization. In *Proceedings of 3rd International Conference on Learning Representations (ICLR)*, San Diego, California, 2015.
- Kiyono, S., Kobayashi, S., Suzuki, J., and Inui, K. SHAPE: Shifted absolute position embedding for transformers. In Moens, M.-F., Huang, X., Specia, L., and Yih, S. W.-t. (eds.), *Proceedings of the 2021 Conference on Empirical Methods in Natural Language Processing*, pp. 3309–3321, Online and Punta Cana, Dominican Republic, November 2021. Association for Computational Linguistics. doi: 10.18653/v1/2021.emnlp-main.266.
- Klimesch, W. Memory processes, brain oscillations and EEG synchronization. *International Journal of Psychophysiology*, 24(1):61–100, 1996. ISSN 0167-8760. doi: 10.1016/S0167-8760(96)00057-8. New Advances in EEG and cognition.
- Laje, R. and Buonomano, D. V. Robust timing and motor patterns by taming chaos in recurrent neural networks. *Nature Neuroscience*, 16(7):925–933, 2013. doi: 10.1038/nn.3405.
- Lillicrap, T. P. and Santoro, A. Backpropagation through time and the brain. *Current Opinion in Neurobiology*, 55:82–89, 2019. ISSN 0959-4388. doi: 10.1016/j.conb.2019.01.011. Machine Learning, Big Data, and Neuroscience.
- Lillicrap, T. P., Cownden, D., Tweed, D. B., and Akerman, C. J. Random synaptic feedback weights support error backpropagation for deep learning. *Nature Communications*, 7(1):13276, 2016. doi: 10.1038/ncomms13276.
- Loshchilov, I. and Hutter, F. SGDR: stochastic gradient descent with warm restarts. In *Proceedings of the 5th International Conference on Learning Representations (ICLR)*. OpenReview.net, 2017.
- Maass, W., Natschläger, T., and Markram, H. Real-time computing without stable states: A new framework for neural computation based on perturbations. *Neural Computation*, 14(11):2531–2560, 2002. doi: 10.1162/089976602760407955.
- Marder, E. and Bucher, D. Central pattern generators and the control of rhythmic movements. *Current Biology*, 11(23):R986–R996, 2001. doi: 10.1016/S0960-9822(01)00581-4.
- Matell, M. S. and Meck, W. H. Cortico-striatal circuits and interval timing: coincidence detection of oscillatory processes. *Cognitive Brain Research*, 21(2):139–170, 2004. ISSN 0926-6410. doi: 10.1016/j.cogbrainres.2004.06.012. Neuroimaging of Interval Timing.
- Mazaheri, A. and Jensen, O. Asymmetric amplitude modulations of brain oscillations generate slow evoked responses. *Journal of Neuroscience*, 28(31):7781–7787, 2008. ISSN 0270-6474. doi: 10.1523/JNEUROSCI.1631-08.2008.
- Merker, B. Cortical gamma oscillations: the functional key is activation, not cognition. *Neuroscience & Biobehavioral Reviews*, 37(3):401–417, 2013. ISSN 0149-7634. doi: 10.1016/j.neubiorev.2013.01.013.
- Miall, C. The storage of time intervals using oscillating neurons. *Neural Computation*, 1(3):359–371, 09 1989. ISSN 0899-7667. doi: 10.1162/neco.1989.1.3.359.
- Mildenhall, B., Srinivasan, P. P., Tancik, M., Barron, J. T., Ramamoorthi, R., and Ng, R. NeRF: Representing scenes as neural radiance fields for view synthesis. In Vedaldi, A., Bischof, H., Brox, T., and Frahm, J.-M. (eds.), *Proceedings of the European Conference on Computer Vision (ECCV)*, pp. 405–421, Cham, 2020. Springer International Publishing. ISBN 978-3-030-58452-8. doi: 10.1007/978-3-030-58452-8_24.

- Milner, P. M. A model for visual shape recognition. *Psychological Review*, 81(6):521–535, 1974. ISSN 0033-295X. doi: 10.1037/h0037149.
- Neil, D., Pfeiffer, M., and Liu, S.-C. Phased lstm: Accelerating recurrent network training for long or event-based sequences. In Lee, D., Sugiyama, M., Luxburg, U., Guyon, I., and Garnett, R. (eds.), *Advances in Neural Information Processing Systems*, volume 29. Curran Associates, Inc., 2016.
- Nikulin, V. V., Linkenkaer-Hansen, K., Nolte, G., Lemm, S., Müller, K. R., Ilmoniemi, R. J., and Curio, G. A novel mechanism for evoked responses in the human brain. *European Journal of Neuroscience*, 25(10):3146–3154, 2007. doi: 10.1111/j.1460-9568.2007.05553.x.
- Nikulin, V. V., Linkenkaer-Hansen, K., Nolte, G., and Curio, G. Non-zero mean and asymmetry of neuronal oscillations have different implications for evoked responses. *Clinical Neurophysiology*, 121(2):186–193, 2010. ISSN 1388-2457. doi: 10.1016/j.clinph.2009.09.028.
- Nyhus, E. and Curran, T. Functional role of gamma and theta oscillations in episodic memory. *Neuroscience & Biobehavioral Reviews*, 34(7):1023–1035, 2010. ISSN 0149-7634. doi: 10.1016/j.neubiorev.2009.12.014. Binding Processes: Neurodynamics and Functional Role in Memory and Action.
- Paszke, A., Gross, S., Chintala, S., Chanan, G., Yang, E., DeVito, Z., Lin, Z., Desmaison, A., Antiga, L., and Lerer, A. Automatic differentiation in PyTorch. In *NIPS Autodiff Workshop*, 2017.
- Paszke, A., Gross, S., Massa, F., Lerer, A., Bradbury, J., Chanan, G., Killeen, T., Lin, Z., Gimelshein, N., Antiga, L., Desmaison, A., Kopf, A., Yang, E., DeVito, Z., Raison, M., Tejani, A., Chilamkurthy, S., Steiner, B., Fang, L., Bai, J., and Chintala, S. PyTorch: An imperative style, high-performance deep learning library. In Wallach, H., Larochelle, H., Beygelzimer, A., d’Alché Buc, F., Fox, E., and Garnett, R. (eds.), *Advances in Neural Information Processing Systems*, volume 32, pp. 8024–8035. Curran Associates, Inc., 2019.
- Perez-Orive, J., Mazor, O., Turner, G. C., Cassenaer, S., Wilson, R. I., and Laurent, G. Oscillations and sparsening of odor representations in the mushroom body. *Science*, 297(5580):359–365, 2002. doi: 10.1126/science.1070502.
- Proctor, J., Kukillaya, R. P., and Holmes, P. A phase-reduced neuro-mechanical model for insect locomotion: feed-forward stability and proprioceptive feedback. *Philosophical Transactions of the Royal Society A: Mathematical, Physical and Engineering Sciences*, 368 (1930):5087–5104, 2010. doi: 10.1098/rsta.2010.0134.
- Rahaman, N., Baratin, A., Arpit, D., Draxler, F., Lin, M., Hamprecht, F., Bengio, Y., and Courville, A. On the spectral bias of neural networks. In Chaudhuri, K. and Salakhutdinov, R. (eds.), *Proceedings of the 36th International Conference on Machine Learning*, volume 97 of *Proceedings of Machine Learning Research*, pp. 5301–5310. PMLR, 09–15 Jun 2019.
- Ruoss, A., Delétang, G., Genewein, T., Grau-Moya, J., Csordás, R., Bennani, M., Legg, S., and Veness, J. Randomized positional encodings boost length generalization of transformers. In Rogers, A., Boyd-Graber, J., and Okazaki, N. (eds.), *Proceedings of the 61st Annual Meeting of the Association for Computational Linguistics (Volume 2: Short Papers)*, pp. 1889–1903, Toronto, Canada, July 2023. Association for Computational Linguistics. doi: 10.18653/v1/2023.acl-short.161.
- Seth, A. K., McKinsty, J. L., Edelman, G. M., and Krichmar, J. L. Visual binding through reentrant connectivity and dynamic synchronization in a brain-based device. *Cerebral Cortex*, 14(11):1185–1199, 11 2004. ISSN 1047-3211. doi: 10.1093/cercor/bhh079.
- Shadlen, M. N. and Movshon, J. A. Synchrony unbound: A critical evaluation of the temporal binding hypothesis. *Neuron*, 24(1):67–77, 2024/01/28 1999. doi: 10.1016/S0896-6273(00)80822-3.
- Shaw, P., Uszkoreit, J., and Vaswani, A. Self-attention with relative position representations. In *Proceedings of the 2018 Conference of the North American Chapter of the Association for Computational Linguistics: Human Language Technologies, Volume 2 (Short Papers)*, pp. 464–468, New Orleans, Louisiana, June 2018. Association for Computational Linguistics. doi: 10.18653/v1/N18-2074.
- Shi, X., Chen, Z., Wang, H., Yeung, D.-Y., Wong, W.-k., and WOO, W.-c. Convolutional LSTM network: A machine learning approach for precipitation nowcasting. In Cortes, C., Lawrence, N., Lee, D., Sugiyama, M., and Garnett, R. (eds.), *Advances in Neural Information Processing Systems*, volume 28. Curran Associates, Inc., 2015.
- Siegelmann, H. T. Recurrent neural networks and finite automata. *Computational Intelligence*, 12(4):567–574, 1996. doi: 10.1111/j.1467-8640.1996.tb00277.x.
- Siegelmann, H. T. *Neural Networks and Analog Computation: Beyond the Turing Limit*. Birkhauser Boston Inc., Cambridge, MA, USA, 1999. ISBN 0-8176-3949-7.
- Siegelmann, H. T. and Sontag, E. D. On the computational power of neural nets. In *Proceedings of the Fifth Annual Workshop on Computational Learning Theory*,

- COLT '92, pp. 440–449, New York, NY, USA, 1992. Association for Computing Machinery. ISBN 089791497X. doi: 10.1145/130385.130432.
- Siegelmann, H. T. and Sontag, E. D. Analog computation via neural networks. *Theoretical Computer Science*, 131(2):331–360, 1994. ISSN u. doi: 10.1016/0304-3975(94)90178-3.
- Siegelmann, H. T. and Sontag, E. D. On the computational power of neural nets. *Journal of Computer and System Sciences*, 50(1):132–150, 1995. ISSN 0022-0000. doi: 10.1006/jcss.1995.1013.
- Song, T., Sun, J., Zhang, Y., and Peng, W. An RNN model for generating sentences with a desired word at a desired position. *Technical Gazette*, 27(1):81–88, February 2020. ISSN 1848-6339. doi: 10.17559/tv-20190929153200.
- Song, Y., Sohl-Dickstein, J., Kingma, D. P., Kumar, A., Ermon, S., and Poole, B. Score-based generative modeling through stochastic differential equations. In *9th International Conference on Learning Representations, ICLR 2021, Virtual Event, Austria, May 3-7, 2021*. OpenReview.net, 2021.
- Stam, C. J., Vliegen, J. H. R., and Nicolai, J. Investigation of the dynamics underlying periodic complexes in the eeg. *Biological Cybernetics*, 80(1):57–69, 1999. doi: 10.1007/s004220050504.
- Sundermeyer, M., Schlüter, R., and Ney, H. LSTM neural networks for language modeling. In *Proceedings of INTERSPEECH*, pp. 194–197, 2012. doi: 10.21437/Interspeech.2012-65.
- Teyler, T. J. and DiScenna, P. The hippocampal memory indexing theory. *Behavioral Neuroscience*, 100(2):147–154, 1986. ISSN 0735-7044. doi: 10.1037/0735-7044.100.2.147.
- Vaswani, A., Shazeer, N., Parmar, N., Uszkoreit, J., Jones, L., Gomez, A. N., Kaiser, L. u., and Polosukhin, I. Attention is all you need. In Guyon, I., Luxburg, U. V., Bengio, S., Wallach, H., Fergus, R., Vishwanathan, S., and Garnett, R. (eds.), *Advances in Neural Information Processing Systems 30*, pp. 5998–6008. Curran Associates, Inc., 2017.
- Vincent-Lamarre, P., Lajoie, G., and Thivierge, J.-P. Driving reservoir models with oscillations: a solution to the extreme structural sensitivity of chaotic networks. *Journal of Computational Neuroscience*, 41(3):305–322, 2016. doi: 10.1007/s10827-016-0619-3.
- Voelker, A., Kajić, I., and Eliasmith, C. Legendre memory units: Continuous-time representation in recurrent neural networks. In Wallach, H., Larochelle, H., Beygelzimer, A., d'Alché-Buc, F., Fox, E., and Garnett, R. (eds.), *Advances in Neural Information Processing Systems*, volume 32. Curran Associates, Inc., 2019.
- von der Malsburg, C. The correlation theory of brain function. In Domany, E., van Hemmen, J. L., and Schulten, K. (eds.), *Models of Neural Networks: Temporal Aspects of Coding and Information Processing in Biological Systems*, pp. 95–119. Springer New York, New York, NY, 1981/1994. ISBN 978-1-4612-4320-5. doi: 10.1007/978-1-4612-4320-5_2. Originally published as Internal Report 81-2, Dept. of Neurobiology, Max-Planck-Institute for Biophysical Chemistry, Göttingen, Germany.
- Wehr, M. and Laurent, G. Odour encoding by temporal sequences of firing in oscillating neural assemblies. *Nature*, 384(6605):162–166, 1996. doi: 10.1038/384162a0.
- Weiss, G., Goldberg, Y., and Yahav, E. On the practical computational power of finite precision rnns for language recognition. In *Proceedings of the 56th Annual Meeting of the Association for Computational Linguistics (Volume 2: Short Papers)*, pp. 740–745. Association for Computational Linguistics, 2018.
- Zugaro, M. B., Monconduit, L., and Buzsáki, G. Spike phase precession persists after transient intrahippocampal perturbation. *Nature Neuroscience*, 8(1):67–71, 2005. doi: 10.1038/nn1369.

A. hyperparameters

Across the experiments, the dimensionality of the hidden layer of the RNNs was set to 512. The embedding of the input integers and the memory cell of the LSTM also had the same dimensionality of 512.

The models were trained for 300,000 iterations using the Adam optimizer (Kingma & Ba, 2015) with the parameters $(\beta_1, \beta_2) := (0.9, 0.999)$ and no weight decay. The learning rate was linearly warmed up from 0.0 to 0.001 for the first 1,000 iterations, and then annealed according to the cosine schedule (Loshchilov & Hutter, 2017). The batch size was 512.

All the experiments were implemented in PyTorch (ver. 2.1.1; Paszke et al., 2017; 2019) and each training-test trial was executed on a single NVIDIA A100 GPU (with 80GB VRAM) hosted by the ACCMS, Kyoto University.

B. Supplementary Results on Reverse Ordering

This section reports supplementary results on the reverse-ordering task (§4).

B.1. Input Sequences of Variable Length

In §4, the reverse-ordering task was performed on fixed-length inputs ($L = 64$). One might think that positional encoding is *exceptionally* effective under this setting, informing RNNs with the exact timing when each input token should be returned as the output. Thus, it remains unclear whether or not position-encoded RNNs can also handle a larger vocabulary even when the input length is variable and, thus, the exact timing of the output emission is *not* identifiable from the positional encoding attached to the inputs.

To assess the robustness against perturbations in the input length, an additional experiment was conducted on the LSTM, with the input length varied between 32 and 64. In this setup, the maximum input length ($= 64$) covers the entirety of the shortest input sequence plus its reversed reconstruction ($= 32 + 32$). Consequently, the positional encoding per se cannot even distinguish the input vs. output phases at $t = 33, \dots, 64$. The vocabulary size was set to 16,384.

As a result, the positional encoding still improved the LSTM’s performance on the reverse-ordering task against the perturbations in the input length (Fig. 6). This result suggests that the effectiveness of the positional encoding for RNNs is not limited to strictly scheduled tasks.

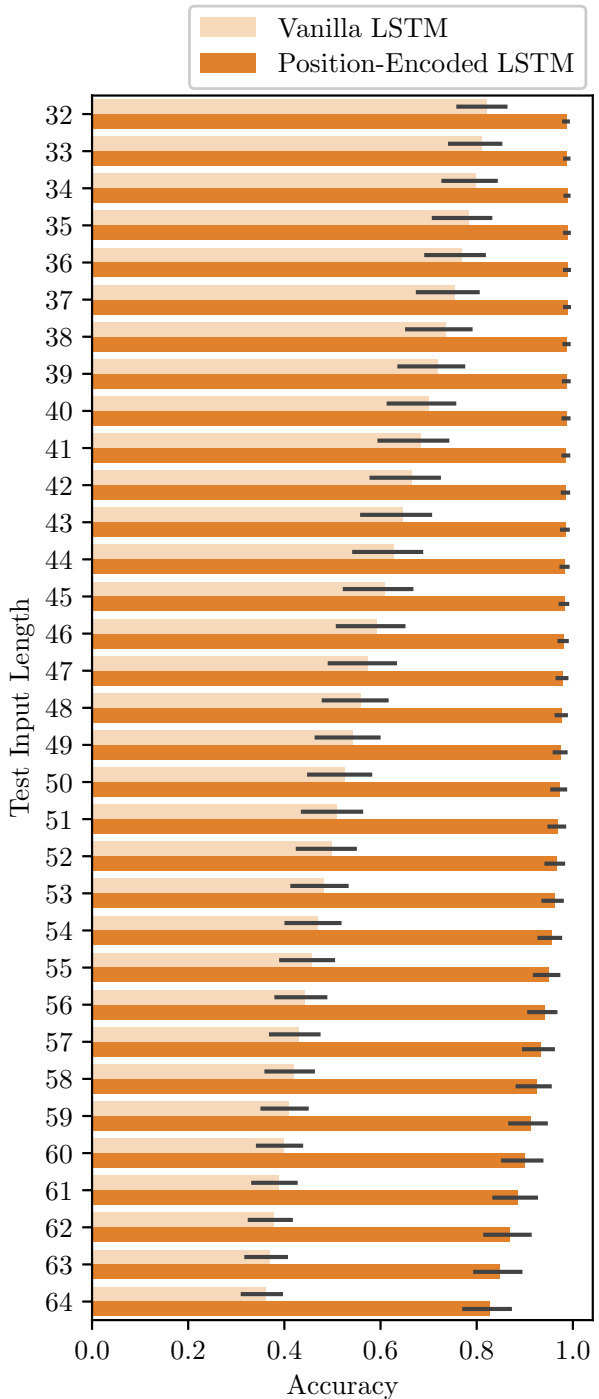


Figure 6. Token-wise accuracy of the reverse-ordering task performed by the LSTM with and without positional encoding (labeled as “Position-Encoded” and “Vanilla” respectively). During training, the input length was randomly selected from a range of 32 to 64. The vocabulary size was set to 16,384. The error bars represent the 95% confidence interval estimated from 10,000 bootstrapped samples of five training-test trials with different random seeds. Each of the five trials held out 1024 random sequences per length for computing the test accuracy.

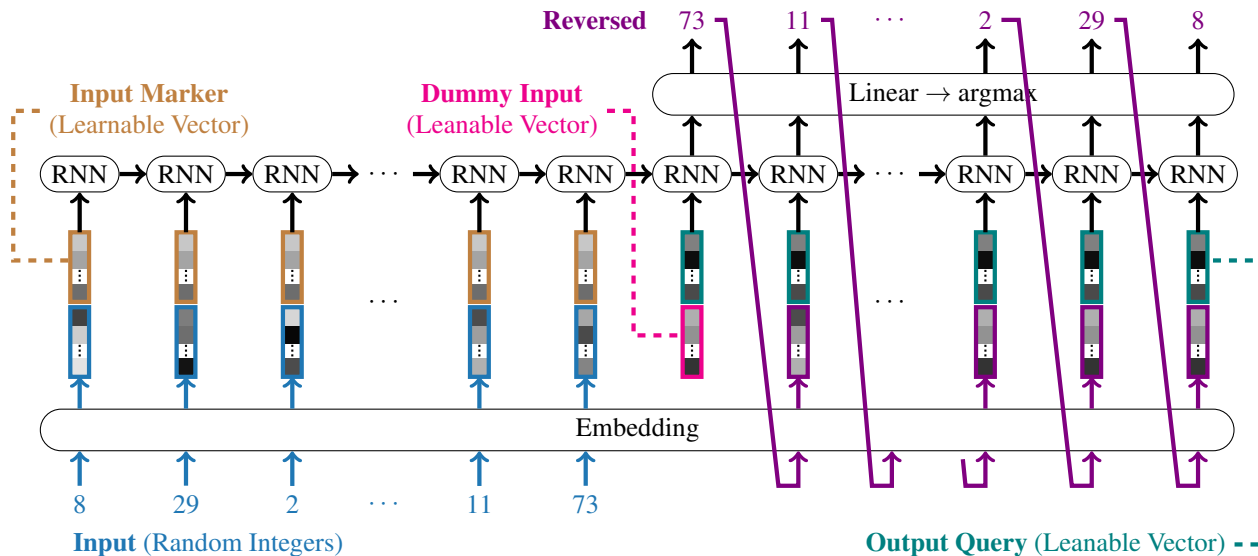


Figure 7. Autoregressive model for the reverse-ordering task.

B.2. Autoregressive Model

Generative models of time series data typically takes advantage of *autoregression*; their prediction made at time t is fed back as (a part of) their input for the next time step $t + 1$. Autoregression is especially helpful when the generative process is stochastic and also dependent on the record of previous outputs—as most famously demonstrated by language models—because a complex joint probability distribution over sequences, $P(x_1, \dots, x_T)$, can be decomposed into the product of the conditional probability of each token, $\prod_{t=1}^T P(x_t | x_1, \dots, x_{t-1})$ (chain rule).

The reverse-ordering task, on the other hand, uses i.i.d. random tokens for the network inputs and the output targets are deterministic. Therefore, the models do *not* enjoy the probabilistic advantage of autoregression. Nevertheless, autoregression can still help RNNs update their internal state by telling them which tokens have already been processed and are thus “forgettable”.

Accordingly, an autoregressive LSTM was benchmarked on the reverse-ordering task (Fig. 7). During the output phase, the model prediction was fed back to the input-embedding layer. The embeddings were shared between the input and output phases, and additional learnable vectors were concatenated with them in order to distinguish the two phases. For the initial prediction, a dummy token was fed to the network in place of the feedback.

It is worth noting that the self-feedback to the autoregressive model was substituted with the ground-truth output during its training (as in other studies). In other words, the model was trained as if it *never* produced any prediction error, and only encountered erroneous feedbacks in the testing phase.

And it was this discrepancy between the training and testing conditions that constrained the performance of the autoregressive model (Fig 8). Although the pseudo feedback of the ground-truth outputs helped reduce the training loss and achieved higher accuracy than the non-autoregressive model (without positional encoding), the accuracy of the true autoregression with self-feedback remained low when the vocabulary size was large.

Incorrect predictions by an autoregressive model magnify errors in the future time steps when they are fed back to the model. By contrast, positional encoding is unaffected by the model predictions (or input values) and thus exhibits greater stability than autoregression.

B.3. Exploration of an “Infinite” Vocabulary

The present study revealed that position-encoded RNNs can handle a larger vocabulary than vanilla networks. A natural inquiry stemming from this finding is *What happens when the vocabulary size goes to infinity?*

To address the question, learning of an “infinite” vocabulary was tested. Uniformly random input tokens were drawn from the unit hypersphere of $8 - 1$ to $512 - 1$ dimensions, and the input embedding was replaced by a linear projection to the input space of the RNN module (of 512 dimensions, as noted in Appendix A). The RNN layer operated in the same way as with the finite vocabularies, and the output-projection layer returned point predictions—instead of probability distributions—of the input tokens in reverse order. The training objective was to maximize the cosine similarity.

In contrast to the experiments conducted with finite vocabularies, the results showed no discernible effect of positional

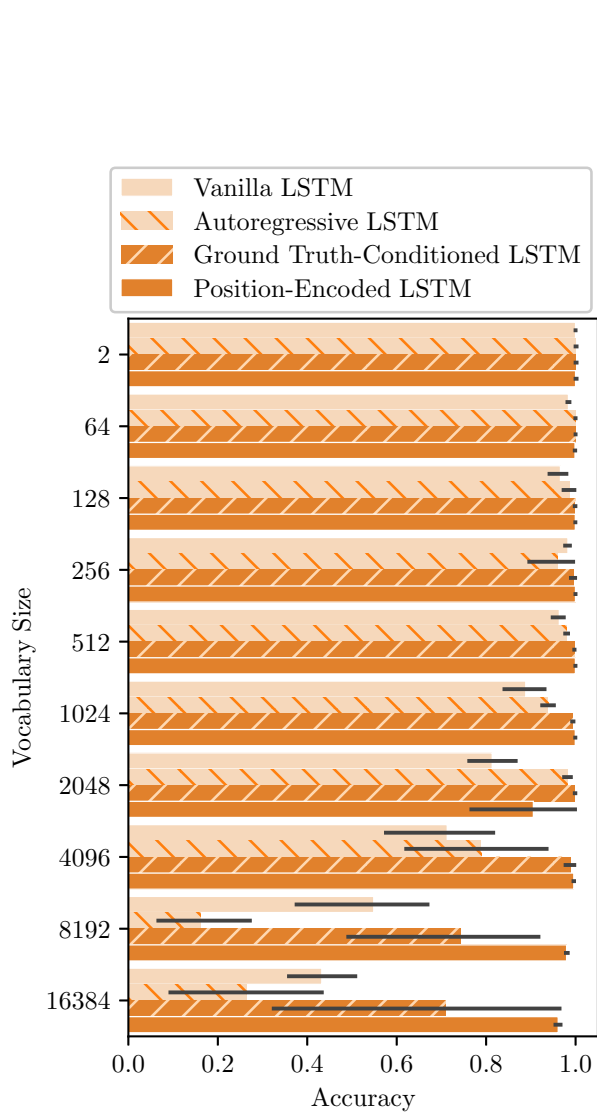


Figure 8. Token-wise accuracy of the reverse-ordering task performed by the autoregressive LSTM. The accuracy is reported based on both self-feedback and ground-truth feedback (labeled as “Autoregressive” and “Ground Truth-Conditioned” respectively). For easier comparison, the results from the vanilla and position-encoded LSTMs (Fig. 2) were repeated. The input length was fixed at 64. The error bars represent the 95% confidence interval estimated from 10,000 bootstrapped samples of five training-test trials with different random seeds. Each of the five trials held out 1024 random sequences per length for computing the test accuracy.

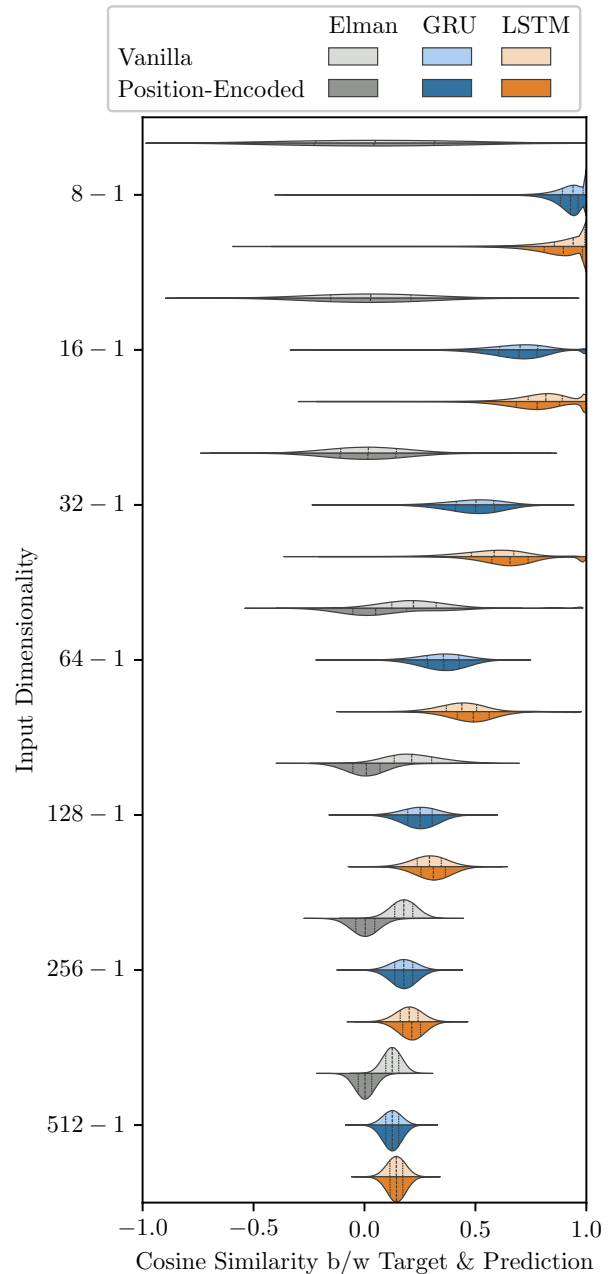


Figure 9. Distributions of the cosine similarity between random input vectors drawn from the unit hypersphere of 8–512 dimensions and their reconstructions by RNNs with and without positional encoding (labeled as “Position-Encoded” and “Vanilla” respectively). The learning objective of the networks was also maximization of the cosine similarity. The input length was fixed at 64. Each distribution was estimated from five networks trained with different random seeds, each of which predicted 1024 sequences (i.e., $5 \times 1024 \times 64 = 327,680$ tokens in total). The vertical dashed lines inside the plots denote the 25, 50, and 75 percentiles from the left to right.

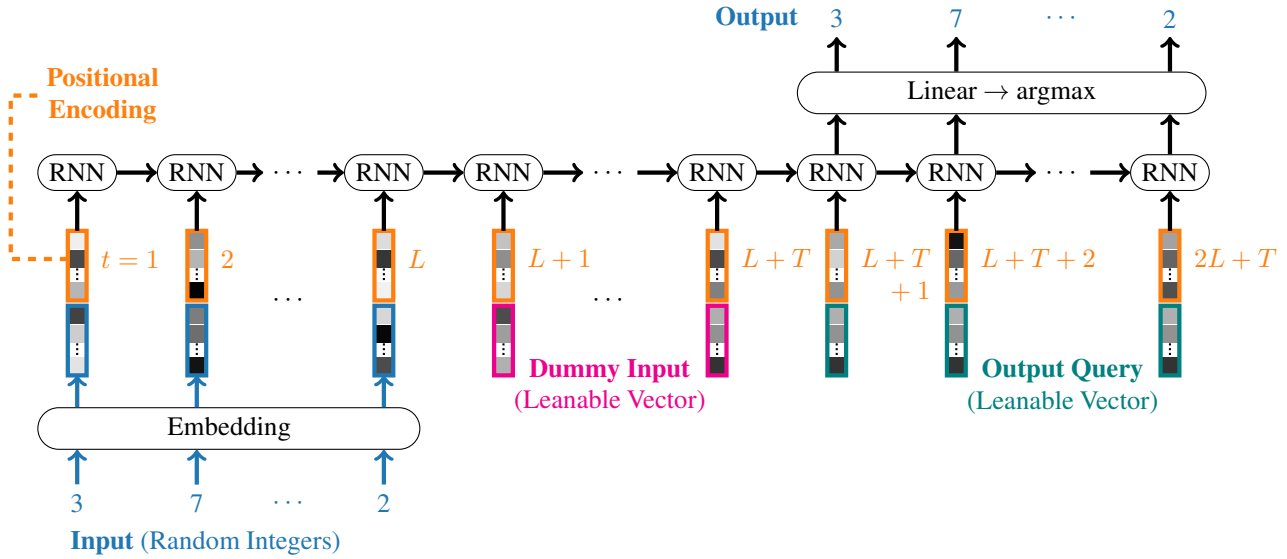


Figure 10. Schematic illustration of the copying memory task.

encoding on the reverse ordering of random spherical vectors. The prediction accuracy of the GRU and LSTM (measured by the cosine similarity) decreased as the dimensionality of the hypersphere increased, regardless of whether the positional encoding was used or not. The positional encoding degraded the performance of the Elman RNN for the high-dimensional inputs (64–512).

C. Other Tasks

This section reports the effect of positional encoding on two additional tasks other than the reverse-ordering task discussed in the main text.

C.1. Copying Memory Task

As discussed in §2.1, the copying memory task (Fig 10) stands as the gold standard benchmark for assessing the memory duration of RNNs (Arjovsky et al., 2016; Neil et al., 2016; Chang et al., 2017; Jing et al., 2017; 2019; Voelker et al., 2019; Gu et al., 2020). This section investigates whether positional encoding also influences RNNs in this task.

The experiment was conducted on the LSTM network. Following the previous studies (Arjovsky et al., 2016; Neil et al., 2016; Chang et al., 2017; Jing et al., 2017; 2019; Voelker et al., 2019; Gu et al., 2020), the input length and the vocabulary size were set to 10 and 8 respectively. The time steps of the “hold” phase—during which the model received dummy inputs, and did nothing but maintained the memorized information against decay—ranged from 60 to 100.

As a result, the positional encoding did not improve the

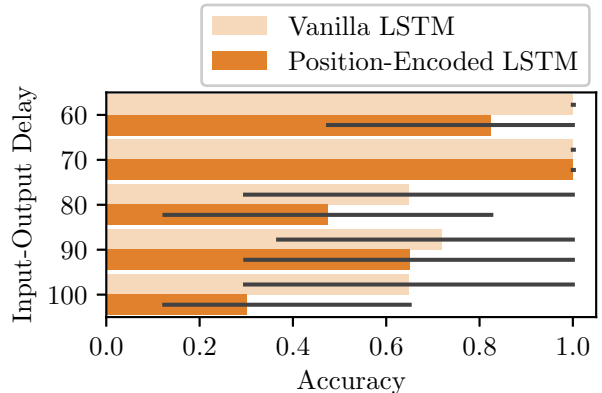


Figure 11. Token-wise accuracy of the copying memory task performed by the LSTM with and without positional encoding (labeled as “Position-Encoded” and “Vanilla” respectively). The input length and the vocabulary size were set to 10 and 8 respectively, following the previous studies (Arjovsky et al., 2016; Neil et al., 2016; Chang et al., 2017; Jing et al., 2017; 2019; Voelker et al., 2019; Gu et al., 2020). The error bars represent the 95% confidence interval estimated from 10,000 bootstrapped samples of five training-test trials with different random seeds. Each of the five trials held out 1024 random sequences per length for computing the test accuracy.

the performance on the task (Fig. 11). The wide error bars in the figure indicate that the learning was unstable, irrespective of whether the LSTM was position-encoded; the model either attained the perfect accuracy or got stuck at the chance level (≈ 0.125).

This experiment revealed that the positional encoding does not extend the memory duration of RNNs. Taken together with the other results reported here, the positive contribution of the positional encoding seems to be limited to the manageability of larger vocabularies.

C.2. Sorting Task

The other additional task was to simply sort the input integers in their inherent ascending order (e.g. 8, 29, 2, 11 \mapsto 2, 8, 11, 29). Thus, the order of input observations was completely irrelevant; this benchmark investigated the effect of positional encoding on the acquisition of “lexicalized” information of input tokens, whereas the scope of the reverse-ordering task in the main text centered on learning of “syntactic” rules invariant to input values.

The input integers were uniformly randomly sampled *with* replacement, allowing for ties in the sorting process.

As a result, positional encoding also proved effective for RNNs to handle a larger vocabulary in the sorting task (Fig. 12), though the improvement remained marginal compared to the reverse-ordering task. While the accuracy declined as the vocabulary size increased beyond 512—regardless of whether the positional encoding was employed—the position-encoded GRUs and LSTMs were more tolerant of the large vocabularies than those without positional encoding. Position-encoded Elman RNNs also displayed a slight improvement at the vocabulary size of 64 (2.09 points on average).

The cause of the prediction errors was further investigated by checking if the model outputs were sorted in ascending order, ignoring whether or not these predictions matched the target sequences. And it was discovered that over 99.9% of the model predictions were indeed sorted as desired, regardless of the use/non-use of positional encoding and RNN types (even the Elman RNN returned sorted predictions, without losing output variations). Hence, the prediction errors were attributed to incorrect construction of the inventory of input values, or misretrieval from the inventory.

It is noteworthy that autoregression is considered effective in this sorting task, in principle, because the feedback of the previous outputs can narrow down the range of possible successors (which are lower-bounded by the latest output). In reality, however, autoregression suffered again from the discrepancy between the ground-truth feedback in the training phase and the self-feedback in the testing phase (Fig. 13); incorrect self-feedback induced further errors in

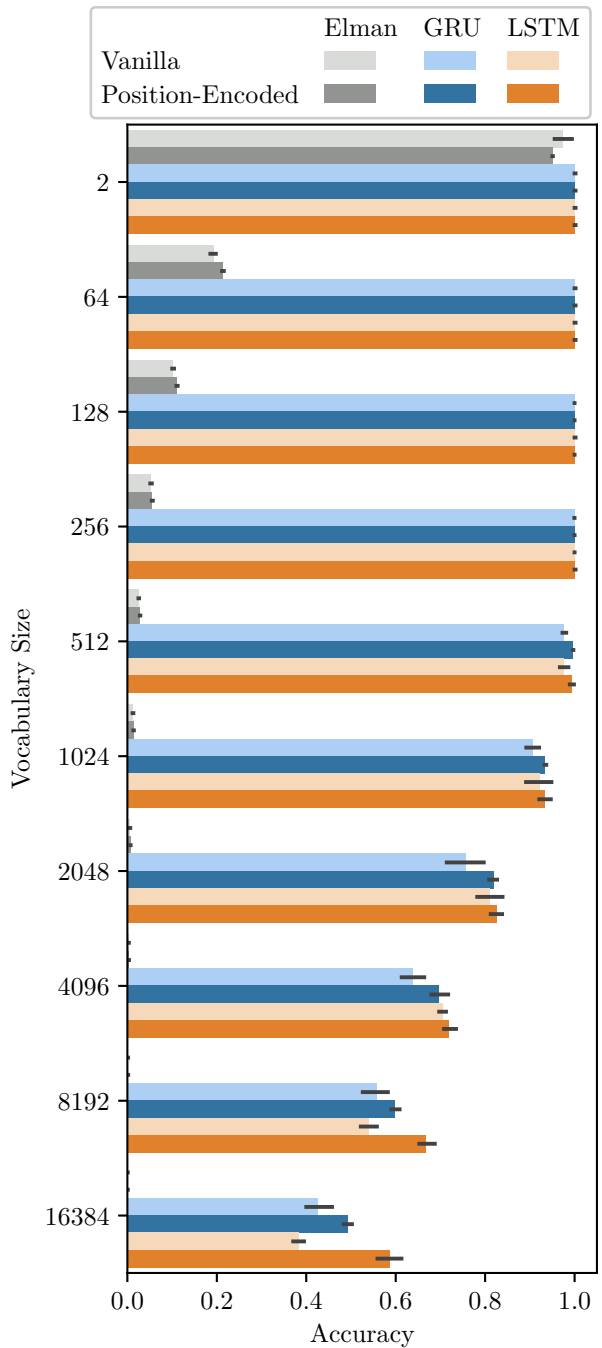


Figure 12. Token-wise accuracy of the sorting task performed by RNNs with and without positional encoding (labeled as “Position-Encoded” and “Vanilla” respectively). The input length was fixed at $L := 64$. The error bars represent the 95% confidence interval estimated from 10,000 bootstrapped samples of five training-test trials with different random seeds. Each of the five trials held out 1024 random sequences (= 65,536 tokens) for computing the test accuracy.

future predictions. Hence, positional encoding is again a more stable enhancer for RNNs than autoregression.

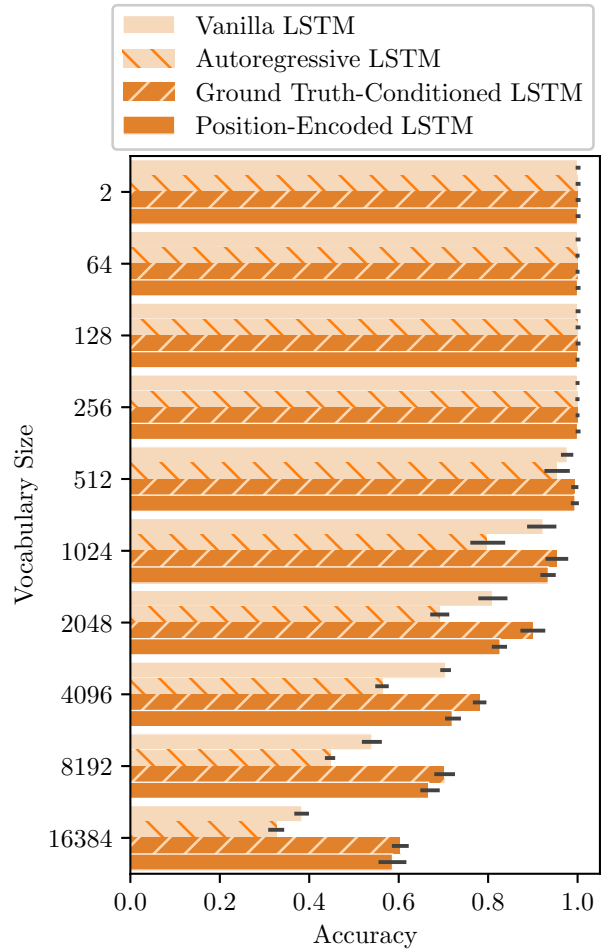


Figure 13. Token-wise accuracy of the sorting task performed by the autoregressive LSTM. The accuracy is reported based on both self-feedback and ground-truth feedback (labeled as “Autoregressive” and “Ground Truth-Conditioned” respectively). For easier comparison, the results from the vanilla and position-encoded LSTMs (Fig. 12) were repeated. The input length was fixed at 64. The error bars represent the 95% confidence interval estimated from 10,000 bootstrapped samples of five training-test trials with different random seeds. Each of the five trials held out 1024 random sequences per length for computing the test accuracy.